In "Fire and Mud: Eruptions and Lahars of Mount Pinatubo, Philipp
Edited by C.G. Newhall and R.S.Punongbayan (1997)
Univ. Washington Press, Seattle.

Occurrence and Origin of Sulfide and Sulfate in the 1991 Mount Pinatubo Eruption Products

By Keiko Hattori[1]

ABSTRACT

Sulfide phases are found in a wide variety of the 1991 eruption products from Mount Pinatubo. Sulfides in early-formed phenocrysts (olivine and augite) in basalt fragments and dome-forming andesite are globular nickel-bearing pyrrhotite, whereas some sulfides in the glass are irregularly shaped and copper rich. Sulfides in dacitic pumice are mostly copper-rich sulfides (chalcopyrite, $CuFeS_2$, with or without an exsolution product of bornite, Cu_5FeS_4). These sulfides in dacitic pumice contain significant Zn (up to 1.3 weight percent), Se, Ag, As, and Cd. Sulfides in the glass of dacitic pumice exhibit desulfidation reaction rims.

Anhydrite is commonly surrounded by the matrix glass in gray, white, and banded pumice. Smooth contact between the anhydrite and glass confirms that the dacitic melt was in equilibrium with anhydrite immediately before eruption.

The occurrence of sulfide globules in the eruption products indicates that an immiscible sulfide liquid formed in silicate melts and that the melts were once reduced, with an oxygen fugacity below the redox boundary of dissolved sulfur. Later formation of anhydrite in dacitic melt requires an addition of sulfur and oxidation of the magma. It is proposed that supercritical fluid released from ascending mafic melt beneath Mount Pinatubo provided volatile elements and sulfur. Sulfur that discharged from the hot dry melt was mostly SO_2. The reduction of sulfur to H_2S in the cool (~800°C), wet dacite caused oxidation of this dacitic magma. H_2S formed in this way was initially precipitated in the dacite as sulfide minerals together with other volatile elements. Continued influx of SO_2 led oxidation of the dacite and an increase in the sulfur solubility of the melt, which caused partial resorption of sulfide minerals and led to excess sulfur, which was precipitated as anhydrite. The proposed model is consistent with compositions of iron-titanium oxides, abundant fluid inclusions in phenocrysts, high contents of volatile elements and hydrophyllic metals in sulfides, strontium isotopic compositions of anhydrite, and sulfur isotopic values of the bulk rocks.

[1]Ottawa-Carleton Geoscience Centre, *and* Department of Geology, University of Ottawa, Ottawa, Ontario, K1N 6N5, Canada.

INTRODUCTION

The eruption of Mount Pinatubo in June, 1991, introduced ~20 Mt SO_2 into the stratosphere and had a significant effect on the global climate (Bluth and others, 1992; Grant and others, 1992; Gleason and others, 1993). The sulfur-rich nature of the magma is reflected in the occurrence of anhydrite phenocrysts in dacitic pumices (Bernard and others, 1991). Several models have been proposed for the origin of this sulfur, including incorporation of subducted sulfide-sulfate deposits on the East China plate (Whitney, 1992), assimilation of sulfide deposits from the underlying Zambales Ophiolite Complex (Fournelle, 1991), assimilation of hydrothermal sulfate in preexisting volcanic rocks (McKibben and others, 1992; this volume), and the introduction of sulfur gases from underlying mafic magma (Pallister and others, 1992; Matthews and others, 1992). Discussions on the origin of sulfur are so far based mostly on chemical and isotopic data for bulk rocks. This paper describes the occurrence and composition of sulfur-bearing phases in various types of eruption products with an emphasis on sulfide minerals and proposes a model for the formation of high-sulfur dacitic magma at Pinatubo.

SAMPLE DESCRIPTION

The 1991 eruption products are dacitic pumice, dome-forming andesite, and basalt. The latter two are volumetrically insignificant, but they are important because they provide evidence supporting an injection of mafic melt as a trigger of the eruption of a semi-solidified dacitic magma (Pallister and others, 1992; Matthews and others, 1992). Basalt commonly occurs as angular to rounded inclusions in andesite that range in diameter from several centimeters to meters. Small inclusions of basalt (<5 cm) are rarely found in gray pumice.

Samples used for this study include six of white pumice; six of gray pumice, three of banded pumice, nine of dome andesite, and four of basalt enclosed in andesites. Three to 10 thin and thick polished sections were made from each sample. The usage of gray and white pumice follows the description by Pallister and others (1992); "gray" pumice actually varies from gray to tan. White pumice is well vesiculated, porphyritic, and contains coarse plagioclase and hornblende phenocrysts. Inclusions are rare, but angular fragments of gray pumice are observed. Gray pumice is poorly vesiculated and has phenocrysts that are much smaller than those of the white pumice (<3 mm). Gray pumices are typically heterogeneous in texture, containing different types of fragments including white pumice, andesite, basalt, and hydrothermally altered volcanic rocks. The altered volcanic fragments do not contain glass, show extensive biotitization and silicification, and appear to have been derived from old volcanic rocks. The banded pumice contains alternating layers of various thickness (1 cm to several centimeters wide) of white pumice and gray pumice; boundaries between bands may be sharp or diffused, and some show intricate mingling textures. Gray layers contain both olivine and hornblende, and they are interpreted to be gray pumice because of the presence of plagioclase phenocrysts and fine grain size of phenocrysts, similar to that of gray pumice. The lack of calcic rims and dusty zones in the plagioclase phenocrysts and the absence of plagioclase microlites argue against an alternative possibility—that the gray layers are andesite—because calcic rims, dusty zones, and microlites are common in the plagioclase population of the dome-forming andesite. Volcanic bombs are usually gray pumice, and one such bomb (~25 cm long) of gray pumice was also examined in this study.

Our samples include two white pumice and one gray pumice specimens collected shortly after the eruption in June 1991 and one specimen of 1991 andesite dome collected along the Maraunot River in the spring of 1992. The rest of the samples were collected in August 1992. Most andesites and basalts were collected along the Maraunot River, ~4 km west of the caldera wall, and one of the basalt samples was from a fragment more than 2 m in diameter, which contains angular andesite fragments. Most pumice samples were collected along the Sacobia River near the upper end of Clark Air Base. There are no apparent differences in mineralogy and textures of samples collected in 1991 and 1992. Anhydrite is well preserved in pumice and andesite samples collected in August 1992. Good preservation of anhydrite in samples collected in 1992 was unexpected, because heavy rainfall in the area could have leached anhydrite from the volcanic rocks, as observed at El Chichón (Luhr and others, 1984). Its preservation at Pinatubo may be attributed to short exposure time of samples at the surface as a result of the daily occurrences of lahars, which continuously brought buried eruption products to the surface.

The 1991 eruption also ejected older volcanic rocks. All samples, however, have been identified with confidence as products of the 1991 eruption because of their highly angular shape and large sizes and the lack of evidence of weathering and devitrification in the glass. Older eruption products are commonly semirounded, and they show various degrees of cloudiness of matrix glass due to devitrification and nucleation of fine dusts of hematite, and Fe-Ti oxide microphenocrysts usually show well-developed exsolution lamellae.

ANALYTICAL PROCEDURES

Major chemical compositions of sulfides were determined by use of a JEOL 6400 digital scanning electron microprobe (SEM), which has a 40° take-off angle for X-rays and is interfaced to a Link X-ray analyzer system (eXL LZ5). Analytical conditions were 20 kV accelerating potential, 39 mm distance between the specimen and the analyzer, 0.8 nA absorbed current on a Faraday cup, and a counting time of 140 to 200 s. Raw X-ray spectra were reduced to elemental concentrations by use of Link ZAF4-FLS analytical software. Analytical standards were natural pyrite for Fe and S, chalcopyrite for Cu, Ni metal for Ni, Co metal for Co, and synthetic ZnS for Zn. Analyses are believed to be accurate to ±2 percent of the amount present; detection limits are ~0.1 percent.

More than 200 grains of sulfides were subjected to probe analysis, but it was difficult to obtain satisfactory analytical results for all grains because of their small size (less than several micrometers in diameter) and interference from the host phases. The compositions of representative sulfides that are large enough to provide quantitative data are given in table 2.

Trace elements of sulfides in thick sections (~100 μm) were determined by a proton-induced X-ray emission microprobe (PIXE). The analytical technique for trace elements in sulfide minerals has been well established (Cabri and others, 1984; Campbell and others, 1989; Czamanske and others, 1992). Operating conditions are similar to those of earlier workers; 3 meV of proton energy, 45° take-off angle, ~8 nA of specimen current, 600 to 900 s counting time, and 4×5 μm beam size. Aluminum absorbers 249 and 352 μm thick were used for pyrrhotite and copper-rich sulfides, respectively. A synthetic pyrrhotite standard (in wt%; Fe=60.93, S=38.87, Se=0.09, and Pd=0.11) was used for calibration. X-rays were detected by a Kevex silicon detector fitted with a beryllium proton shield of 50 μm thick, and data reduction of the raw X-ray spectra were performed by the GUPIX program of Maxwell and others (1989). Detection limits are three times the errors obtained from the background.

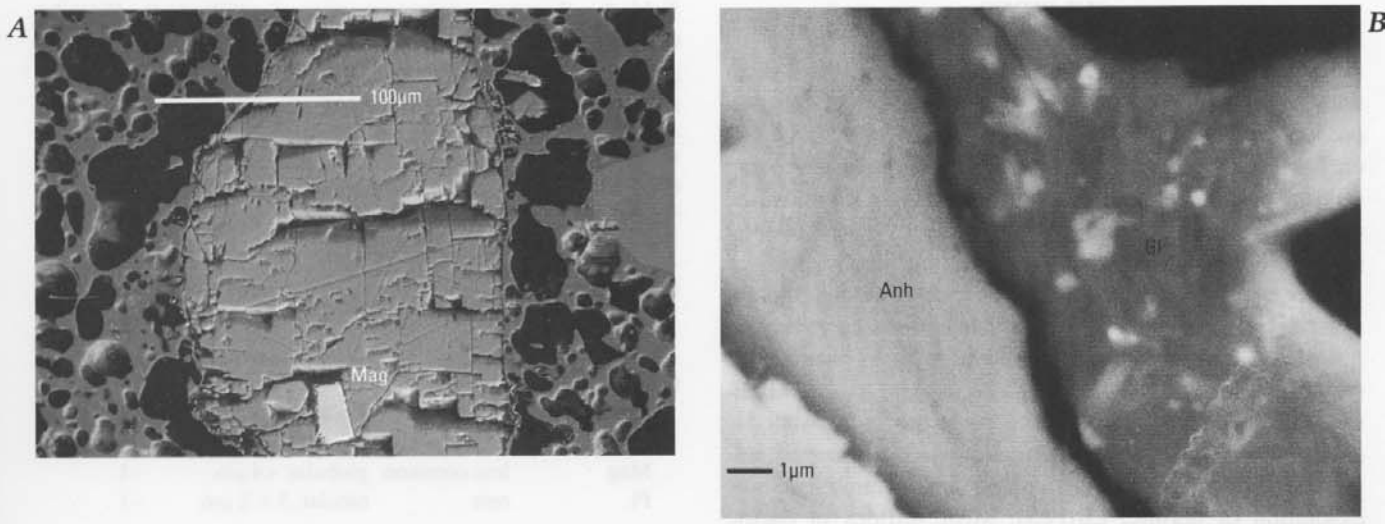

Figure 1. Back-scattered electron images of anhydrite in pumice. *A*, Anhydrite enclosing low-titanium magnetite (Mag) in banded pumice. *B*, Contact between anhydrite (Anh) and glass in white pumice. Note smooth boundary between the two phases. White specks in glass are microphenocrysts.

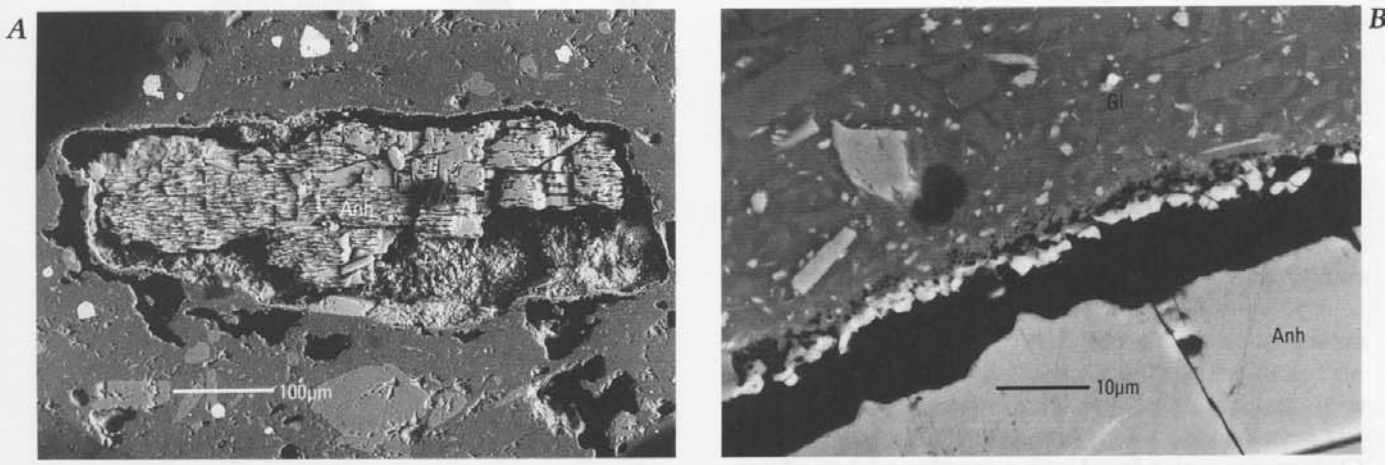

Figure 2. Back-scattered electron images of anhydrite (Anh) in dome andesite. *A*, The reaction rim, only 10 μm wide, is well exposed in the lower right because anhydrite was plucked out during the section preparation (sample CN1B–C). *B*, Boundary between anhydrite (Anh) and glass (Gl) in sample 92814–01B. Minute minerals between glass and anhydrite are apatite, calcite, calcic plagioclase and other calc-silicate minerals. Most of them are plucked out during the section preparation.

OCCURRENCE OF SULFUR PHASES

ANHYDRITE

The occurrence of anhydrite in dacitic pumice has been reported by Knittel and others (1991), Bernard and others (1991), Pallister and others (1991, 1992), and others. This study confirmed its common occurrence in gray and white pumice from Pinatubo. Banded pumice also contains anhydrite in both gray and white pumice layers. Anhydrite crystals are commonly coarse, <0.6 mm, and some grains enclose microphenocrysts of apatite and low-Ti (<1 wt% TiO_2) magnetite (fig. 1*A*). In all pumice samples, the contact between the grains and glass is smooth and there is no evidence of reactions between the two phases (fig. 1*A*,*B*), confirming that anhydrite was a stable liquidus phase in the dacitic melt immediately before eruption. An anhydrite inclusion in hornblende was reported by Fournelle (1991), but none were observed during this study, so it is suggested that such occurrences are extremely rare.

Anhydrite grains up to 0.4 mm in length also occur in the dome andesite. These grains display reaction rims, several micrometers wide along the contact with glass, of calcite, apatite, calcic plagioclase, and other calc-silicates (fig. 2*A*,*B*). Quantitative determination of these phases was impossible because of their small sizes, <0.5 μm.

SULFIDES

All sulfide grains are fine grained and are found in all sections examined in this study, from a variety of eruption products. Occurrences are summarized in table 1. Grains enclosed in phenocrysts are usually small, rarely exceeding 40 μm, but one globular sulfide of cubanite composition (~120 μm) was found in unexsolved rhombohedral ilmenite-hematite solid solution ($ilmenite_{ss}$; fig. 3). Sulfides in the eruption products display four different shapes: spherical or globular sulfide enclosed in phenocrysts and glass (figs. 3, 4), symplectic minute droplets in phenocrysts (fig. 5), and irregular-shaped sulfides in glass (fig. 6). Globular sulfides and symplectic droplets in basalt and andesite are mostly Ni-pyrrhotite, whereas irregularly shaped sulfides in glass contain high copper and commonly show exsolution of bornite, Cu_5FeS_4. Most sulfides in dacitic pumice, independent of shapes and host phases, are Cu-rich sulfides. Several sulfide grains in phenocrysts occur together with glass inclusions (fig. 7).

Basalt.—Sulfide grains are relatively common in basalt fragments in the dome andesite. Phenocrysts of olivine, clinopyroxene, hornblende, $ilmenite_{ss}$, and ulvöspinel-magnetite solid solution ($magnetite_{ss}$) contain sulfides; inclusions in olivine are extremely rare, but a few inclusions were observed. Most sulfides in phenocrysts are small (<10 μm), globular, Ni-bearing pyrrhotite with low copper (<0.1 wt%) (fig. 5). Spherical nickel-bearing pyrrhotite also occurs in the glass (fig. 8). These occurrences suggest that a sulfide liquid had the composition of Ni-Fe monosulfide solid solution. Copper-bearing pyrrhotite and an exsolution product of cubanite ($CuFe_2S_3$) occur in apparently late phenocryst phases, such as $magnetite_{ss}$ and hornblende, which rims olivine. Copper-rich sulfides (atomic ratio of Cu/Fe >1) are not common in basalts and are only found in glass. Chalcopyrite is also found with a complex mixture of iron-rich orthopyroxene and magnetite that appears to replace Ni-pyrrhotite and olivine (fig. 9).

Andesite.—The dome andesite contains sulfides and anhydrite. Sulfides are similar to those of basalt; these sulfides are usually small (<20 μm), but some are ~0.1 mm (fig. 3). Sulfides occur in olivine, augite, hornblende, and oxides ($ilmenite_{ss}$, $magnetite_{ss}$), K-feldspar (confirmed with electron microprobe), and glass. Sulfides in augite, hornblende, oxides are mostly globular Ni-bearing pyrrhotite. Some in hornblende rimming olivine and oxides are copper bearing. One grain of Ni-pyrrhotite in $magnetite_{ss}$ is surrounded by perovskite, possibly a reaction product (fig. 10).

Several Ni-pyrrhotite grains in phenocrysts are replaced by copper-rich sulfide along cleavages and cracks (fig. 11). Sulfides in glass have angular to irregular shapes and they are all copper rich (chalcopyrite with or without exsolution of bornite) (fig. 12). It is common to find pyrrhotite only in phenocrysts and chalcopyrite only in glass (fig. 13). The occurrences and phases of sulfides demonstrate that early sulfides are Ni-pyrrhotite and late sulfides are Cu-sulfides.

Table 1. Summary of the occurrence of sulfides in the Pinatubo eruption products.

[Chr, chromite; Cpx, augite; Hbl, hornblende; Il, ilmenite-hematite solid solution; K-fs, K feldspar; Mag, titanomagnetite (ulvöspinel-magnetite solid solution); Ol, olivine; Qtz, quartz. Most sulfides in the gray pumice were small and analyses were qualitative—adequate to identify the species (below) but not good enough for inclusion in table 2]

Host	Abundance of sulfides in the host	Shape of sulfides	Cu/Fe atomic ratio of bulk composition of S-phase[1]
Gray pumice			
Glass	very rare	angular	~1
Hbl	minor	globular, <5 μm	~1
Mag	less common	globular, <4 μm	~1
Pl	rare	tabular, 3 × 8 μm	~1
White pumice			
Glass	minor	irregular, <40 μm with reaction rim.	>1
Hbl, Mag.	minor	globular, <14 μm	~1, 0
Qtz	rare	angular, <20 μm	>1
Pl	minor	angular, <10 μm	>1, ~1
Banded pumice			
Glass	minor	irregular, <30 μm with reaction rim.	0, ~1
Hbl	minor	globular, <15 μm	0
Mag	minor	globular, angular	0, >1
K-fs	minor	irregular	~1
Andesite			
Glass	minor	angular	~1, >1
K-fs	minor	angular	~1
Hbl	common	globular	0–1
Il	minor	globular	0–1
Mag	common	globular	0–1
Cpx	not common	globular	0
Ol	rare	globular	0
Chr	none		
Basalt			
Glass	common	globular	0
		irregular, <40 μm	>1
Hbl	common	globular	0–1
Il	rare	globular	0–1
Mag	rare	globular	~1
Cpx	rare	globular	0
Ol	rare	globular	0

[1]Grains containing bornite exsolution obviously have Cu/Fe atomic ratios higher than 1. Grains containing cubanite exsolution have the ratio close to 1. The ratios of Fe-sulfides with no exsolution phases are shown as 0, although some contain several wt% Cu.

Dacitic Pumices.—Most sulfide grains in white pumice are rich in copper (Cu/Fe atomic ratio >1) and a high copper phase is formed as an exsolution product (figs. 14,

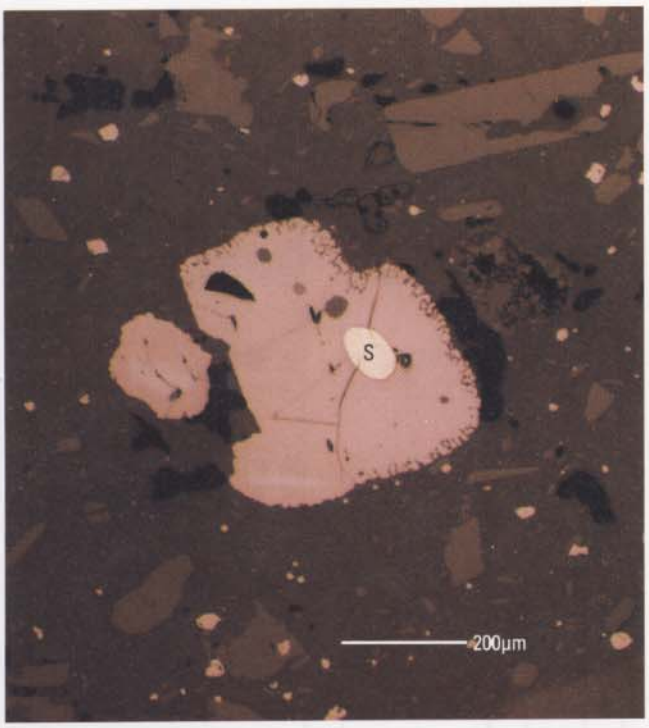

Figure 3. Photomicrograph of a rounded cubanite grain (S; 120 μm long) enclosed in ilmenite$_{ss}$ in dome andesite (sample 920814–10).

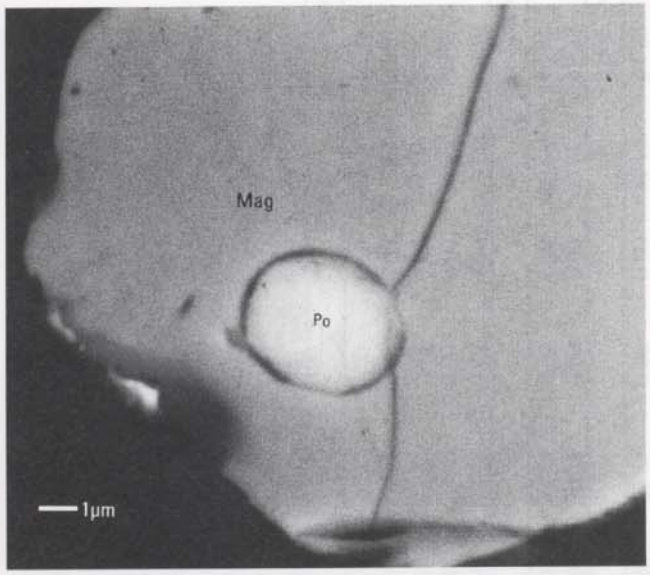

Figure 4. Back-scattered electron image of spherical grain of pyrrhotite (Po) in magnetite$_{ss}$ (Mag) in dome andesite (sample CN1B–C–X).

15). The sulfides were originally formed as a high-temperature Cu-Fe-S intermediate solid solution. Due to their small sizes and fine lamellae width (figs. 14, 15, 16), it was impossible to determine the precise compositions of the Cu-rich phase, but it is likely bornite (Cu_5FeS_4), on the

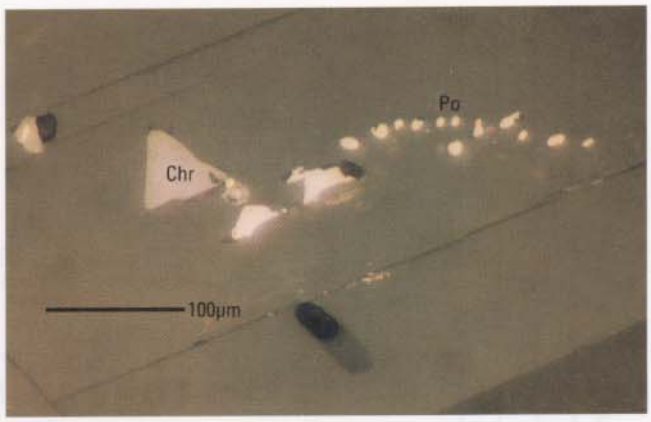

Figure 5. Photomicrograph showing symplectic chains of Ni-bearing pyrrhotite (Po) droplets in hornblende in basalt. Olivine and hornblende commonly enclose chromite (Chr) (sample 920814–11A). Scale bar corresponds to 100 μm.

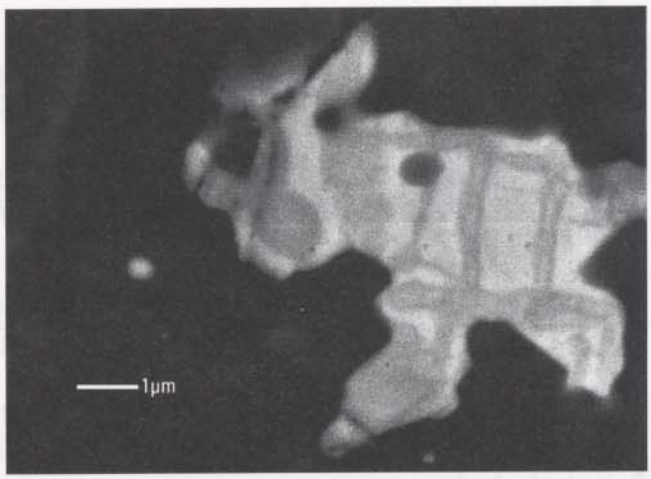

Figure 6. Back-scattered electron image of irregularly shaped sulfide grain containing exsolution product of bornite (bright part) in chalcopyrite (darker matrix) in the glass of dome andesite (sample CN1B–D–C).

basis of the Cu-Fe-S phase relations and the degree of electron back-scattering from the phase. Pyrrhotite is very rare in pumice samples, but rounded grains of pyrrhotite were found within hornblende and magnetite$_{ss}$ phenocrysts in gray pumice.

Sulfides in phenocrysts are usually globular to spherical (fig. 14) and many in plagioclase are angular (fig. 15). Sulfides in matrix glass generally have an angular shape (figs. 16, 17). Some are exceptionally high in copper, forming a bornite matrix with exsolved chalcopyrite inclusions. Several Cu-Fe sulfides in glass are high in zinc, up to 1.3 wt% (table 3). Ni-pyrrhotite grains are extremely rare but are found in gray pumice and in bands of gray pumice within banded pumice. Most sulfide grains enclosed in glass

Table 2. Chemical compositions of representative sulfides in Pinatubo eruption products.

[Cpx, augite; Gl, glass; Hbl, hornblende; Il, ilmenite-hematite solid solution; K-fs, K-feldspar; Mag, ulvöspinel-magnetite solid solution; Ol, olivine; Ox, oxides; Pl, plagioclase]

Sample no	Weight percent							Atomic percent						
	Host	S	Fe	Ni	Co	Cu	Sum	S	Fe	Ni	Co	Cu	Cu/Fe	Remarks
White Pumice														
PP1-A1	Gl	34.83	33.26	0.00	0.00	31.41	99.50	49.92	27.37	0.00	0.00	22.72	0.83	
PP1A-3	Gl	34.35	33.12	0.00	0.00	30.96	98.43	49.79	27.56	0.00	0.00	22.65	0.82	
PP1-A,x	Gl	34.99	33.53	0.00	0.23	30.73	99.48	50.08	27.55	0.00	0.18	22.19	0.81	
10-PP1A4	Gl	35.17	33.43	0.19	0.00	31.71	100.50	49.91	27.23	0.15	0.00	22.71	0.83	
PP1A4	Hbl	36.30	56.83	0.00	0.25	0.65	94.03	52.32	47.02	0.00	0.20	0.47	0.91	
32PP1-BE1	Gl	35.54	41.74	0.00	0.00	21.69	98.97	50.45	34.02	0.00	0.00	15.54	0.46	1.3% Zn
33PP1-BE2	Gl	34.44	40.56	0.00	0.00	19.87	94.76	50.83	34.37	0.00	0.00	14.80	0.43	1.0% Zn
PP2C-B	Pl	31.67	30.43	0.28	0.00	34.24	96.62	47.58	26.24	0.23	0.00	25.95	0.99	
PP2D,B	Pl	31.49	29.98	0.00	0.00	33.81	95.28	47.89	26.16	0.00	0.00	25.95	0.99	
4PP1-C,A	Gl	26.55	14.83	0.00	0.00	55.84	97.22	41.98	13.46	0.00	0.00	44.55	3.31	Cu-rich part of a grain
PP1-C,A	Gl	31.08	27.38	0.00	0.00	37.13	95.59	47.42	23.99	0.00	0.00	28.59	1.19	matrix of the grain
PP1-C	Hbl	35.09	39.47	0.43	0.00	22.50	97.49	50.55	32.65	0.00	0.00	16.36	0.50	
PP1-AD1	Hbl	32.73	33.82	0.31	0.00	31.33	98.19	48.01	28.48	0.24	0.00	23.19	0.81	
PP1-AD2	Hbl	32.72	33.74	0.00	0.00	30.85	97.31	48.36	28.63	0.00	0.00	23.01	0.80	
PP1-AE	Mag	32.88	33.90	0.00	0.00	32.80	99.58	47.72	28.25	0.00	0.00	24.03	0.85	
29PP1BD1	Hbl	33.93	35.56	0.00	0.00	31.74	101.23	48.22	29.02	0.00	0.00	22.76	0.78	
30PP1BA1	Gl	34.30	29.92	0.00	0.00	33.82	98.04	50.04	25.06	0.00	0.00	24.90	0.99	
31PP1BA2	Gl	31.98	29.26	0.00	0.00	33.34	94.58	48.75	25.61	0.00	0.00	25.65	1.00	
Gray Pumice														
511-812-4B	Gl	31.61	30.98	0.00	0.00	32.84	95.53	47.92	26.96	0.00	0.00	25.12	0.93	
513-812-4C	Ox	31.97	35.14	0.00	0.00	30.76	97.87	47.25	29.81	0.00	0.00	29.81	0.77	
Banded pumice														
528-813-17C1	Gl	39.64	61.12	0.00	0.00	0.00	100.76	53.04	46.95	0.00	0.00	0.00	0.00	
536-813-17A1	K-fs	34.42	30.42	0.00	0.00	34.52	99.36	49.67	25.20	0.00	0.00	25.13	1.00	
549-813-17B1	Mag	32.74	33.17	0.44	0.00	32.05	98.41	48.00	27.93	0.35	0.00	23.72	0.85	
529-813-17	Gl	35.68	59.31	0.00	0.00	0.65	95.64	50.93	48.60	0.00	0.00	0.47	0.01	
530-813-17	Gl	34.10	36.38	0.00	0.00	26.94	97.43	49.72	30.45	0.00	0.00	19.82	0.65	
Andesite														
CN1-BD2	Il	27.13	60.04	0.47	0.00	0.75	88.39	43.60	55.39	0.42	0.00	0.59	0.01	
CN1-BB1	Gl	36.18	51.48	1.49	0.00	6.19	95.34	51.93	42.44	1.17	0.00	4.48	0.11	
CN1-BCX	Ox	35.04	55.25	0.29	0.00	3.79	94.37	50.91y	46.09	0.23	0.00	2.77	0.06	
CN1-BB2	Gl	32.05	29.10	0.00	0.00	32.21	93.36	49.30	25.70	0.00	0.00	25.01	0.97	
CN1B-A1	K-fs	34.45	30.35	0.00	0.00	34.48	99.28	49.73	25.15	0.00	0.00	25.11	0.75	
401-814-1BB1	Ol/Hbl	39.65	54.34	4.34	0.00	0.00	98.33	54.16	42.61	3.23	0.00	0.00	0.00	beside chromite
402-814-1BB	Hbl	34.72	35.20	0.43	0.00	28.42	99.18	49.95	29.07	0.00	0.00	20.64	0.71	
404-814-1BB2	Gl	29.03	25.33	0.00	0.00	39.63	94.00	45.66	22.89	0.00	0.00	31.46	1.38	center
405-814-1BB2	Gl	30.00	16.56	0.00	0.00	53.69	100.25	45.05	14.28	0.00	0.00	40.68	2.85	branch part

Table 2. Chemical compositions of representative sulfides in Pinatubo eruption product—Continued

Sample no.	Host	Weight percent						Atomic percent						Remarks
		S	Fe	Ni	Co	Cu	Sum	S	Fe	Ni	Co	Cu	Cu/Fe	
Andesite—Continued														
407-814-1BC	Hbl	33.38	27.83	0.00	0.00	37.27	98.47	48.97	23.44	0.00	0.00	27.59	1.18	
409–814-1BA1	Mg	33.42	38.13	0.00	0.00	28.97	100.51	47.79	31.31	0.00	0.00	20.90	0.67	
412–814-10	Ox	35.64	39.87	0.00	0.00	27.40	102.91	49.26	31.64	0.00	0.00	19.11	0.60	in fig. 3
414-814-10	Mag	32.68	31.76	0.00	0.00	37.95	102.39	46.64	26.05	0.00	0.00	27.33	1.05	
814-10	Mag	34.94	39.09	0.00	0.00	26.86	100.90	48.90	31.40	0.00	0.00	18.97	0.60	
525-814-3D	Gl	34.26	35.69	0.00	0.00	27.95	97.90	49.76	29.75	0.00	0.00	20.49	0.69	branch part
527-814-3B1	Hbl/Gl	34.27	30.69	0.00	0.00	33.97	98.93	49.65	25.52	0.00	0.00	24.83	0.97	
Basalt fragment														
417-814-11BA2	K-fs	39.44	59.69	0.46	0.00	0.74	100.33	53.06	46.10	0.34	0.00	0.50	0.01	
418-814-11BA3	Gl	39.85	58.57	0.00	0.00	0.94	99.36	53.89	45.47	0.00	0.00	0.64	0.01	
419-814-11CA	Hbl	39.29	60.37	1.20	0.00	0.00	100.86	52.67	46.46	0.88	0.00	0.00	0.00	
420-814-11CB	Hbl	37.54	45.93	1.04	0.00	17.10	101.61	51.35	36.07	0.78	0.00	11.71	0.33	
548-814-11A1	Hbl	37.23	57.08	1.62	0.00	2.52	98.45	51.59	45.42	1.23	0.00	1.76	0.04	beside chromite.
549–814-11AB	Cpx	38.93	58.02	1.18	0.00	0.00	98.13	53.41	45.71	0.88	0.00	0.00	0.00	
437-814-2AA	Il	39.05	58.96	1.33	0.00	0.00	99.34	53.04	45.98	0.99	0.00	0.00	0.00	
432–814-2AF	Mag/Gl	30.44	17.02	0.44	0.00	52.24	100.14	45.56	14.63	0.36	0.00	39.45	2.70	Cu-rich part.
431-814-2AE	Mag/Gl	29.54	33.92	0.00	0.00	33.63	97.09	44.77	29.52	0.00	0.00	25.72	0.87	Cu-poor part.
433-814-2AE	Mag/Gl	35.21	31.62	0.00	0.00	35.03	101.86	49.56	25.56	0.00	0.00	24.88	0.97	another part.
435–814-2AD1	Hbl	37.35	48.13	2.80	0.00	8.29	96.57	52.26	38.66	2.14	0.00	5.85	0.15	
436-814-2AD2	Hbl	34.49	37.86	0.71	0.00	23.42	96.48	50.40	31.77	0.56	0.00	17.27	0.54	
434-814-2AB	Ox	36.67	46.37	0.00	0.00	19.48	102.52	50.35	36.41	0.00	0.00	13.44	0.37	

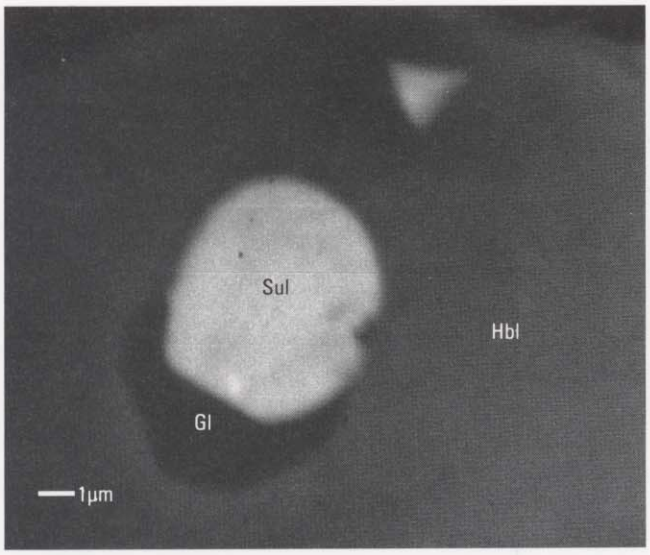

Figure 7. Back-scattered electron image of sulfide inclusions (Sul) in hornblende (Hbl) in white pumice (sample PP1–92526–C). Dark area (Gl) surrounding sulfide contains K, Cl, Al, Si, and Fe, and it is interpreted to be a glass inclusion.

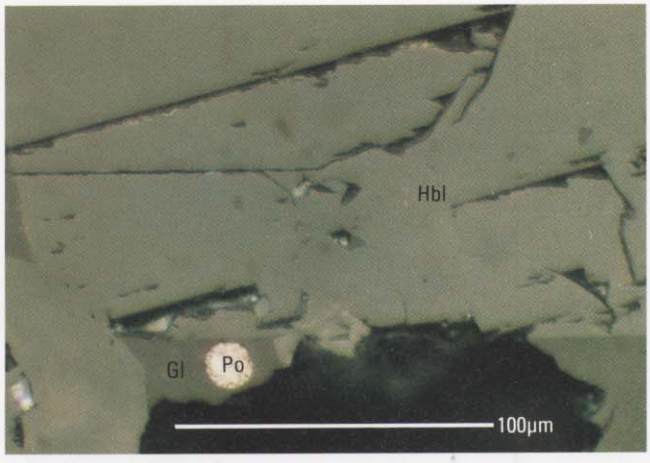

Figure 8. Reflected light photomicrograph of spherical grain of pyrrhotite (Po) in basalt glass (Gl) adjacent to hornblende (Hbl).

show reaction rims that are composed of a fine mixture of oxides and sulfides. The presence of reaction rims reflects desulfidation (figs. 16, 17), which indicates that sulfide was not stable in the dacitic magma immediately before eruption. The narrow width of rims and dispersed occurrences of remnant sulfides prevented their quantitative compositional analysis, but they appear to be fine iron oxides.

Selenium contents of sulfides are high with Se/S ratios in a range of 20×10^{-5} to 100×10^{-5} (table 3). The ratios are slighter higher than the values of meteorites (~33×10^{-5}; Wedephol, 1972), sulfides in mantle xenoliths (~30×10^{-5}; Hattori and others, 1992), and sulfides in midocean ridge

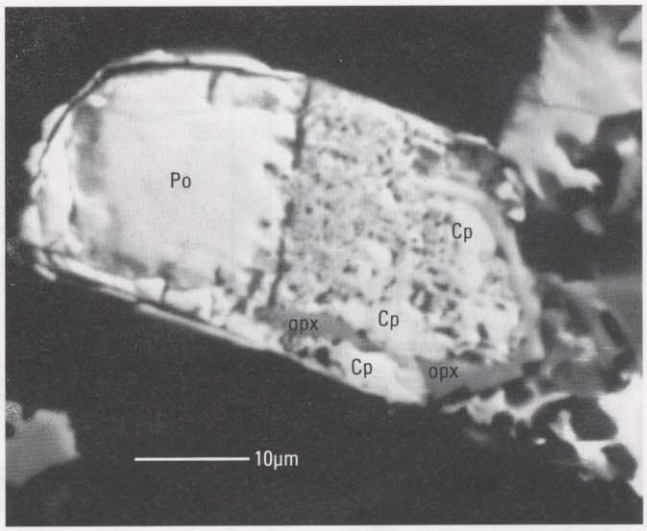

Figure 9. Reflected light photomicrograph of a symplectic mixture of very fine grained magnetite, orthopyroxene (opx) and chalcopyrite (Cp) replacing Ni-bearing pyrrhotite (Po). Quantitative determination of silicate phase (dark part in Po) was difficult because of the small sample size, but the X-ray spectrum suggests it is olivine. Sample (920814–11) is from a large basalt fragment in andesite.

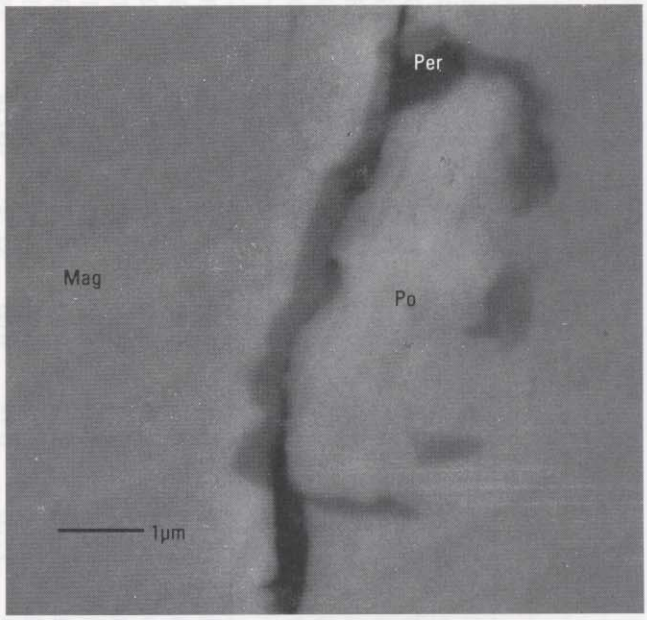

Figure 10. Back-scattered electron image of Ni-bearing pyrrhotite (Po) in magneite$_{ss}$ (Mag). Dark phase between sulfide and oxides is perovskite (Per). Sample (CH1BE–W) is a dome andesite.

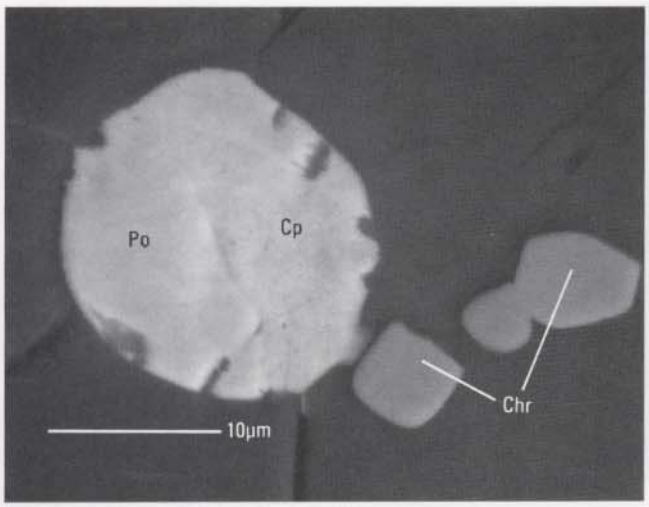

Figure 11. Back-scattered electron image of globular Ni-bearing pyrrhotite (Po), partially replaced by Cu-rich sulfides (Cp) along the cracks of olivine rimmed by hornblende. Chromite (Chr) grains at the right. Note that the rim of pyrrhotite is partially corroded.

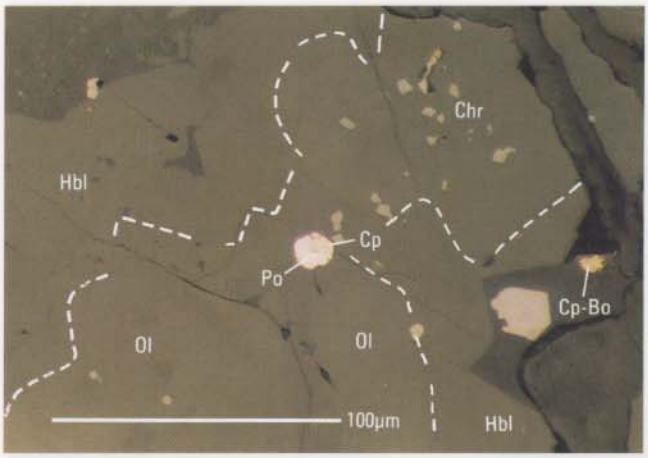

Figure 13. Back-scattered electron image of Ni-bearing pyrrhotite (Po) in olivine (Ol) rimmed by hornblende (Hbl) and Cu-rich sulfides (Cp, Bo) in glass. Minute chromite grains (Chr) are visible in olivines. A closeup view of the Po-Cp grain is shown in figure 11. Scale bar is 200 μm.

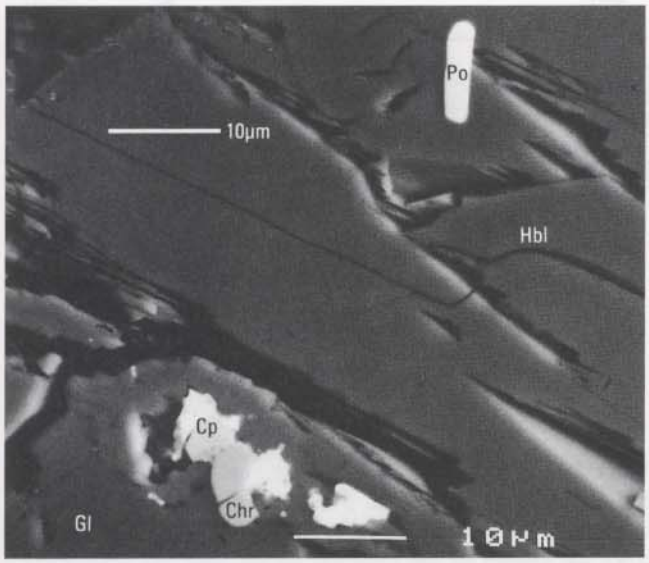

Figure 12. Back-scattered electron image of two kinds of sulfides. Sulfides enclosed in hornblende (Hbl) are rounded Ni-rich pyrrhotite (Po), and sulfides in glass (Gl) are irregularly shaped, Cu-rich sulfide (Cp). Fine grains of chromite (Chr) are common. Sample (CH1BB–A) is dome andesite.

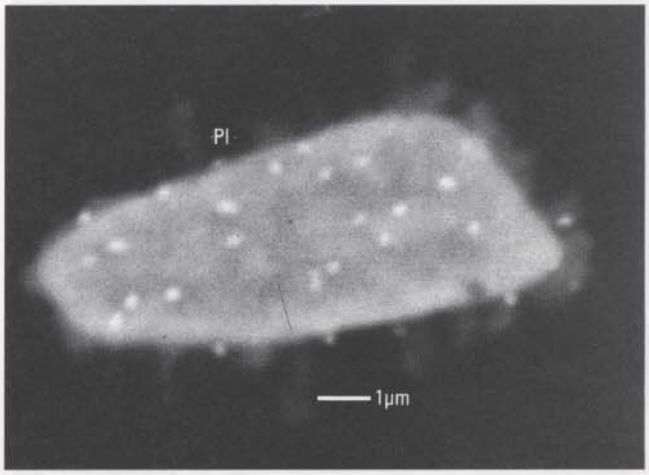

Figure 14. Back-scattered electron image showing typical occurrence of Cu-rich sulfides in white pumice. Sulfides in 2-mm-long plagioclase (Pl) phenocryst. The bright portion is the exsolution product of bornite; the dark portion is chalcopyrite (sample PKN 29–2).

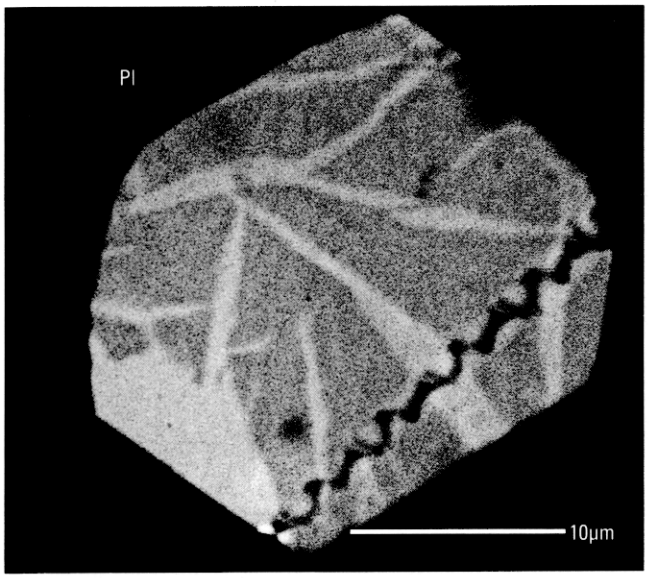

Figure 15. Back-scattered electron image of sulfide in 3-mm-long plagioclase (Pl) phenocryst (sample PP1–C–A).

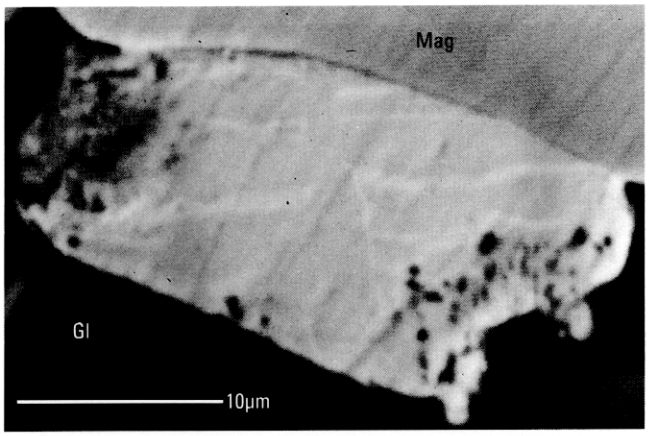

Figure 16. Back-scattered electron image of sulfides showing desulfidization rim around the grain in the glass of white pumice. The sulfide on the contact with magnetite (mag) and glass (Gl) displays exsolution lamellae of bornite (bright) from chalcopyrite (dark) (sample PKN29–2–A).

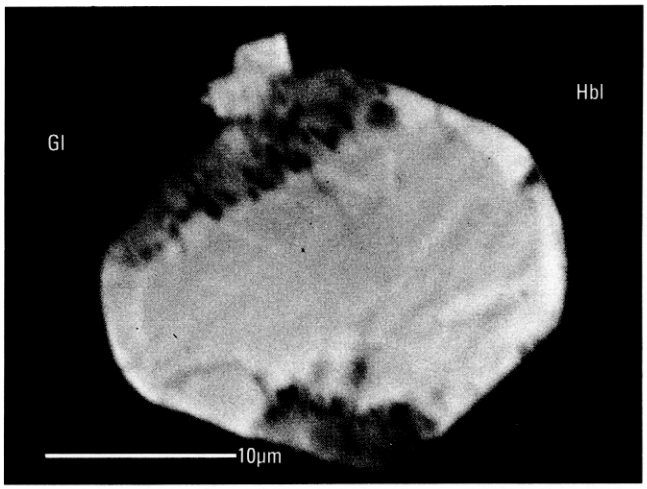

Figure 17. Back-scattered electron image of sulfide in white pumice with oxidized rim (sample PP1–A–A). Gl, glass; Hbl, hornblende.

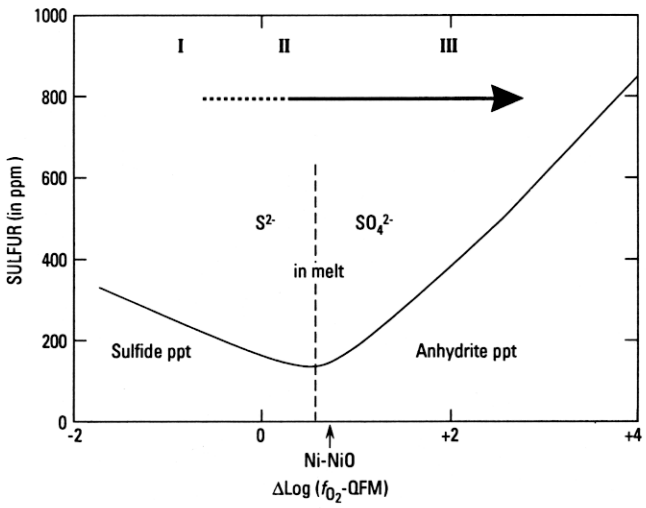

Figure 18. Sulfur solubility in dacitic melt at 900°C (modified after Carroll and Rutherford, 1988). Dotted line is the redox boundary of predominant sulfur species in the melt. Thick arrow shows the change of the Pinatubo dacitic melt. At stage I, an immiscible sulfide liquid forms and scavenges nickel and copper from the silicate melt. At stage II, SO_2 that has been released from mafic melt is reduced to H_2S as it oxidizes the dacitic melt. The added H_2S forms sulfides in the dacitic melt that are high in Cu, Cd, Zn, and Se. At stage III, continuing addition of SO_2 from mafic melt increases f_{O_2} and results in partial desulfidation of previously formed sulfides and precipitation of anhydrite in the dacitic melt. ppm, parts per million; ppt, precipitate.

Table 3. Trace element contents in sulfides in white pumice (in ppm).

Sample	Phase[1]	Host[2]	Zn	As	Se	Mo	Ag	Cd	Sb	Te	S/Se	Se/S × 10^{-5}	Shape
White pumice													
UK29–3	Cp	Gl	2,233	24	314	<6	36	20	<15	35	1,074	93.1	Angular
PP1BB	Cp	Gl	2,569	<8	299	<6	32	24	<16	<22	1,192	83.9	Angular
PP1BB	Cp	Gl	2,884	<9	266	8	10	14	<15	<23	1,244	80.4	Angular
PP1BA	CpB	Gl	212	<3	170	<4	242	42	<22	<34	2,031	49.2	Angular
PP1C,F[3]	Cp	Hbl	1,247	12	61	<5	21	<10	<17	74	2,741	36.5	Globular
PP1A1A[3]	CpB	Gl	2,209	8	276	44	91	22	<18	39	1,501	66.6	Angular
PPA1A[3]	CpB	Gl	2,184	22	333	149	173	16	36	43	1,146	87.3	Angular
Andesite													
4–92814–10C	Cub	Il	919	18	26	<5	unc[4]	30	<25	<35	11,540	8.7	Globular, fig. 3
Basalt fragment													
92814–11AK	CubP	Gl	998	unc[4]	107	<18	<28	<30	62	<60	2,388	41.9	Globular
92814–11AC		Hbl/Gl	536	20	104	<16	25	<35	<47	<70	2,921	34.2	Angular
92814–2BZ	CuPo	Gl	927	41	76	64	46	<35	62	<65	3,778	26.5	Irregular
92814–2BA	CubP	Gl	684	28	78	<16	46	<29	43	<48	4,125	24.2	Irregular
92814–11AD	Po	Hbl	148	13	57	<19	30	<35	<65	<73	5,897	17.0	Globular
92814–11AD	Po	Gl	453	unc[4]	20	26	<17	<14	<29	<36	17,485	5.7	Globular

[1] Sulfide phase: CpB, a mixture of chalcopyrite and exsolution product of bornite; Cp, chalcopyrite; Cub, cubanite; CubP, cubanite-pyrrhotite; CuPo, Cu-bearing pyrrhotite; Po, pyrrhotite.

[2] Phase containing sulfides: Gl, glass; Hbl, Hornblende; Il, unexsolved ilmenite-hematite solid solution.

[3] The grains were too small and the total of Cu, Fe, and S are in a range of 50 to 90%. Trace element concentrations are accordingly normalized.

[4] unc, the presence of the element is uncertain, and the measured concentration is between the detection limit and three times the measurement error.

basalts (~20×10^{-5}; Hamlyn and Keays, 1986; and 30×10^{-5} to 60×10^{-5}; Hattori and others, 1992).

Sulfides in gray phenocryst-poor pumices are rare, but small grains (<1 μm) are found in phenocrysts of magnetite$_{ss}$, hornblende, and plagioclase. Sulfides are extremely rare in the glass of these pumices. Gray pumices with higher phenocryst contents (>10 vol%) contain more sulfide grains than do pumices of the phenocryst-poor variety.

DISCUSSION

SULFUR IN SILICATE MELTS

The solubility of sulfur in silicate melts is controlled by temperature, pressure, oxygen fugacity, and melt composition. The solubility of sulfur at constant temperature is higher in melts with higher iron; mafic melts have a higher solubility of sulfur than less mafic melts (Buchanan and Nolan, 1979). Sulfur in reduced melt is predominantly S^{2-} with minor HS^-, whereas sulfur in oxidized melt is SO_4^{2-} (fig. 18; Katsura and Nagashima, 1974; Carroll and Rutherford, 1988). The redox boundary of dissolved sulfur species, S^{2-} and SO_4^{2-}, is one log f_{O_2} unit above the Ni-NiO (NNO) buffer (Carroll and Rutherford, 1988). At constant temperature and pressure, the solubility of sulfur decreases steadily as f_{O_2} increases up to the redox boundary, and then solubility increases sharply with a further increase in f_{O_2} (fig. 18).

Sulfide liquid formed in mafic silicate melts is enriched in Ni, Co, and Cu because the partition coefficients for these elements between sulfide liquid and silicate melt are high (>250 for Ni and Cu and 50 for Co at 1200°C; Rajamani and Naldrett, 1978). Sulfide liquid that formed in evolved silicate melts tends to be low in nickel and cobalt and high in copper because of preferential incorporation of nickel and cobalt into early silicate minerals.

The evolution of sulfur in the magma may be evaluated from the occurrences of sulfides and anhydrite, assuming that the basalt samples represent mafic melt. Mafic magma was present beneath the dacitic magma chamber shortly before the 1991 eruption (Pallister and others, 1992; Matthews and others, 1992).

SULFUR IN MAFIC MELT AT PINATUBO

Occurrences of globular sulfide grains in phenocrysts and in the glass of basalt fragments suggest that they formed from sulfide liquid and that the mafic melt was saturated with sulfur. Common occurrence of sulfides in oxides is consistent with the experimental results of the solubility of sulfur. Formation of oxides, loss of iron from the melt, probably prompted the separation of sulfide liquid in the silicate melt.

The formation of liquid sulfide in silicate melt indicates that the predominant dissolved sulfur species in the melt was S^{2-} and that the f_{O_2} of the melt was lower than the redox boundary of sulfur species in the melt (f_{O_2} = NNO +1; fig. 18; Nagashima and Katsura, 1973; Carroll and Rutherford, 1988). The mafic magma was not sufficiently oxidized to contain significant SO_4^{2-}, so it could not form anhydrite. The lack of anhydrite in basalt is consistent with this interpretation.

The composition of globular sulfides, Ni-pyrrhotite, indicates that the sulfide liquid was Ni-Fe monosulfide solid solution, similar to most sulfides in many igneous rocks, including midoceanic ridge basalts (Mathez, 1976), oceanic island basalts (Desborough and others, 1968), back-arc basin basalts (Francis, 1990), island arc basalts and andesites (Heming and Carmichael, 1973; Ueda and Itaya, 1981), and continental arc rocks (Anderson, 1974; Whitney and Stormer, 1983).

The contents of copper in the Pinatubo monosulfide solid solution are low, <1 wt%. The low concentration of copper in iron sulfides in the Pinatubo eruption products suggests that the mafic melt was not originally high in copper, as the Cu/Fe ratios of sulfides reflect the ratios of silicate melt. This implies that high copper in later formed sulfides requires a mechanism for the enrichment of copper other than igneous processes.

The Cu/Ni ratio in melts increases during fractional crystallization. Formation of sulfide liquid containing 30 wt% Cu requires a melt with 0.15 wt% Cu, using the partition coefficient for copper between sulfide liquid and silicate melt (Rajamani and Naldrett, 1978). The concentration of copper would not increase to this high level in silicate melts by fractional crystallization alone. If fractional crystallization was the cause, the primary mafic melt should have had exceptionally high copper. As discussed, the possibility is rejected because early-formed sulfides are low in copper. Copper, therefore, must have been added to the mafic melt from an external source after crystallization of these phenocrysts.

The occurrence of highly irregular shaped Cu-rich sulfides in the glass (fig. 6) is very unusual for sulfides in volcanic rocks. The shape suggests that they were not formed as sulfide liquid in a silicate melt. Instead, they formed after the glass was already semisolidified. This interpretation implies that the formation of Cu-rich sulfides may have taken place after the entrapment of mafic melt into the andesitic or dacitic melts.

Fe-Ti oxide assemblages, however, failed to demonstrate reduced f_{O_2} of the mafic melt. The estimated temperatures and f_{O_2} using the solution model by Frost and Lindsley (1992) are similar to those of dacitic melt, ~800°C and two log units above NNO (table 4). The temperatures recorded in oxides are very low for temperatures of mafic magma. Obviously, oxides in basalt have undergone subsolidus equilibration after the entrapment of the magma in cooler

Table 4. Temperature and f_{O_2} estimates from Fe-Ti oxides.

[And, andesite; Bas, basalt; BP, banded pumice; GP, gray pumice; WP, white pumice; Δ_{QFM}, difference between the f_{O_2} and QFM buffer in log units (QFM = quartz-fayalite-magnetite). Contents of Fe_2O_3 and components of ulvöspinel (Usp) and ilmenite (Ilm) calculated using QUILF program by Andersen and others (1993)]

Sample	Rock	SiO_2	Al_2O_3	TiO_2	V_2O_3	FeO	Fe_2O_3	MnO	MgO	Usp	Ilm	Temp. (°C)	Δ_{QFM}
UK29AX	WP	0.00	1.73	4.38	0.48	32.59	52.80	0.43	0.91	0.127		825	+3.1
		.15	.45	28.60	.34	24.32	43.51	.00	.79		0.557		
UK29AY	WP	.09	1.86	4.68	.48	32.83	56.65	.43	1.09	.136		845	+3.0
		.38	.40	28.82	.23	23.44	45.18	.37	1.17		.539		
UK29AZ	WP	.22	1.80	4.58	.44	33.06	56.64	.41	.84	.133		826	+3.1
		.15	.29	28.60	.19	23.82	43.82	.19	.96		.549		
92812–3A	GP	.00	1.92	4.02	.56	32.81	58.16	.00	1.08	.121		817	+3.2
		.00	.66	28.41	.00	23.99	45.08	.00	.88		.547		
92813–01B	GP	.00	2.95	7.24	.25	33.60	50.97	.41	2.25	.215		931	+2.6
(in plagioclase)		.00	.75	29.08	.25	22.92	43.82	.28	1.65		.543		
92813–17E	BP	.00	2.09	4.67	.35	33.42	59.91	.38	1.71	.129		821	+3.1
		.00	.38	29.35	.42	24.43	46.32	.00	1.10		.542		
92814–3C	And	.00	2.10	5.41	.26	33.06	56.32	.55	1.63	.153		856	+2.9
		.00	.51	29.43	.00	24.11	44.57	.00	1.32		.550		
92814–11AF	Bas	.22	1.71	4.00	.36	32.70	58.94	.44	1.00	.113		796	+3.2
		.19	.32	31.36	.00	25.82	40.22	.49	1.06		.590		
92814–11BY	Bas	.00	3.30	11.95	.33	37.63	42.17	.45	2.64	.357		973	+2.0
(in hornblende)		.00	.59	35.75	.00	27.11	33.19	.35	2.62		.648		

andesitic and dacitic magmas. Subsolidus equilibration of oxide composition is known in many slowly cooled igneous rocks (Morse, 1980; Frost and Lindsley, 1991) and experiments have documented fast subsolidus equilibration (Hammond and Taylor, 1982). The once-reduced nature of the mafic melt is, however, evident from low abundances of oxides in basalt. Formation of oxides requires high Fe^{3+}/Fe^{2+}. It is also supported by higher Ti and lower Fe^{2+} of oxides enclosed in phenocrysts (table 4). Phenocryst phases surrounding the oxides prevented them from equilibrating with the matrix glass. Reduced nature of the melt at an earlier time is also supported by the occurrence of a symplectic mixture of magnetite and Fe-rich orthopyroxene, which appear to have replaced pyrrhotite and olivine (fig. 9). The assemblage is indicative of progressive subsolidus oxidation of olivine (Johnston and Stout, 1984).

SULFUR IN DACITIC MELT

Like the mafic melt, the dacitic melt also once had a low f_{O_2} promoting the formation of sulfide liquid during phenocryst crystallization, as documented by globular sulfide inclusions (fig. 18). During that time, sulfur in the melt was predominantly S^{2-}. Fe-Ti oxides again fail to reflect the reduced condition because of later reequilibration of their compositions. They only record the condition just prior to eruption, ~800°C and 3 log units above NNO (table 4). Under this condition, the predominant dissolved sulfur in the melt was SO_4^{2-} (fig. 18) and anhydrite could have formed as a stable phase, as supported by the stable occurrence of anhydrite in the glass (fig. 1A,B).

ORIGIN OF SULFUR AND ANHYDRITE

The solubility of SO_4^{2-} sharply increases with the increase in f_{O_2} (fig. 18). Formation of anhydrite in dacitic melt requires higher concentration of sulfur in the melt than does the formation of sulfide. The relatively reduced nature of the original dacitic melt, indicated by the occurrence of globular sulfides, suggests that the formation of anhydrite in the Pinatubo dacite melt requires two conditions: the oxidation of the residual melt and an addition of sulfur. The addition of sulfur is essential because the silicate melt should have lost much of its sulfur during the transition from the reduced to oxidized state, as the solubility of sulfur in the silicate melt is minimal at the redox boundary (Nagashima and Katsura, 1973). The addition of external sulfur took place during and after crystallization of hornblende, plagioclase, and magnetite, but before the eruption. Most apatite apparently crystallized after oxidation of the residual dacitic melt because apatite in the dacite is high in SO_3, up to 0.8 wt% (Imai and others, 1992; this volume).

Proposed sources of sulfur in high-sulfur magma include (1) subducted seafloor sulfide deposits (Whitney,

1984; 1992), (2) evaporite beds (Rye and others, 1984), (3) sulfide deposits in underlying ophiolite complexes (Fournelle, 1991), (4) sulfate minerals from preexisting volcanic rocks and hydrothermal deposits (McKibben and others, 1992), and (5) SO_2 released from underlying mafic magma (Pallister and others, 1992; Hattori, 1993). High sulfur in the dacitic melt at source (model 1) is not applicable because this study shows that the dacitic magma acquired sulfur from an external source during and after crystallization of phenocrysts. In addition, solubility of sulfur as S^{2-} is lower than the solubility of sulfur as SO_4^{2-} (fig. 18). The content of sulfur in the melt remained low until the melt was oxidized.

Model 2, incorporation of evaporite, proposed for the El Chichón eruption product, is rejected because of the lack of evaporites in the Pinatubo area. There is a thin sequence of Eocene to Pliocene shallow marine sedimentary rocks between the volcanic rocks and Zambales Ophiolite Complex, and the Complex occurs below the sea level beneath the volcano (Delfin, 1984; Delfin and others, this volume). The shallow marine rocks may contain evaporite minerals, but this possibility is discounted for three reasons. First, the assimilation of an evaporite would lower Se/S because of its low Se/S ratios ($<0.1\times10^{-5}$; Measures and others, 1980). Second, evaporites generally contain low amounts of copper. Third, incorporation of young evaporites would raise $^{87}Sr/^{86}Sr$ ratios, given their high $^{87}Sr/^{86}Sr$ (~0.709). The ratios of anhydrite in pumices (0.70421±0.00001; this study) and bulk pumice values (0.70422 to 0.70426; this study) are similar to other volcanic rocks in the Bataan arc (Knittel and others, 1992).

Model 3, incorporation of ophiolite-derived sulfide, is also discounted because it would not provide sulfur with high Se/S and an oxidizing agent for the magma. The two possible sources for additional sulfur that would accompany oxidation of dacitic magma are sulfate minerals from the old volcanic rocks (model 4) and sulfur released from underlying mafic magma (model 5). In either model, sulfur ultimately originated from underlying mafic magma. In the former model (model 4), sulfur was indirectly supplied from the mafic magma to the dacitic melt. This model is appealing, as intense hydrothermal activity had been noted at Pinatubo for a long time. Isotope studies and gas analyses have indicated that the hydrothermal activity was linked to the discharge of volatiles from magma at depth (Ruaya and others, 1992). The preexisting volcanic rocks were extensively altered to form secondary minerals, including anhydrite and sulfides (Delfin, 1984, Delfin and others, this volume; author's examination of Philippine National Oil Company drill chips in 1992). In addition, two porphyry copper deposits that are the product of magmatic-hydrothermal activity (the Dizon mine and Pisumpan deposit; Sillitoe and Gappe, 1984) are located within Mount Pinatubo, and they contain abundant high-temperature hydrothermal anhydrite. Minor porphyry copper deposits might have been present directly beneath the caldera. Assimilation of such rocks into the dacitic magma chamber could have enriched sulfur and oxidized the magma.

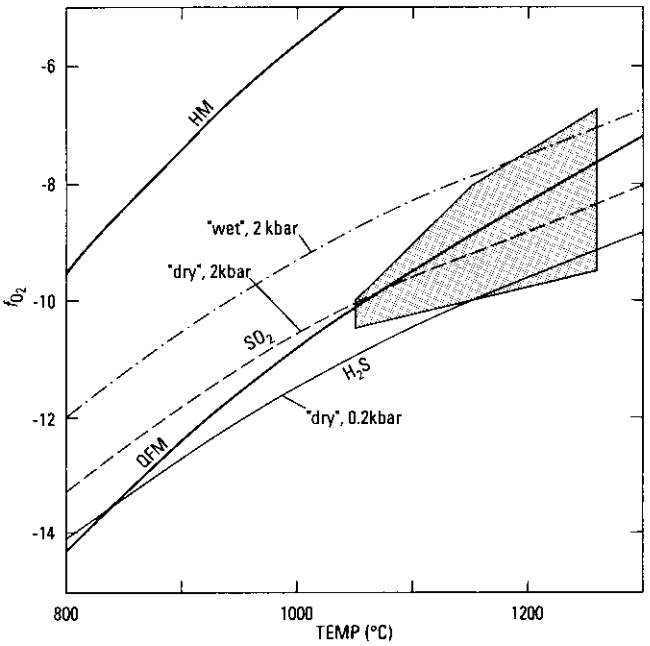

Figure 19. Equal concentrations of SO_2 and H_2S at 200 atm (dashed curve) and 2 kbar (dashed-dotted curve). "Dry" and "wet" fluids have X_{H_2O} 0.01 and 1, respectively, where X is volume ratio. Thick curves are quartz-fayalite-magnetite (QFM) and hematite-magnetite (HM) buffers. Oxidation conditions of mafic melts are shown by the screened area (from Wallace and Carmichael, 1992). Note that fluids released from progressively "drier" and hotter melts have progressively higher SO_2/H_2S ratios.

In the latter model (model 5), sulfur was directly added to the dacitic magma from the underlying mafic melt. The mafic melt at Pinatubo was saturated with sulfur, as evidenced by the occurrences of sulfide globules in phenocrysts. When mafic melt ascends, the vapor phase separates because the solubilities of CO_2 and H_2O decrease with pressure decrease (Holloway, 1976; Burnham and Ohmoto, 1980). Separation of any volatile gases from a melt will cause degassing of other gases, such as H_2S and SO_2, because they have mutual solubilities. For example, degassing of CO_2 or H_2O is accompanied by release of SO_2 from magmas before the saturation of SO_2 itself in the magma because SO_2 will be partitioned to the CO_2 phase from the silicate melt as CO_2 exsolves. Sulfur released from magmas is mostly SO_2 and H_2S. The ratio of SO_2/H_2S of the fluids depends on temperature, f_{O_2}, and f_{H_2O} (fig. 19). That ratio in high-temperature fluids discharged from mafic melts is generally high, as is well documented from volcanic gas data (Gerlach, 1986). H_2S may be predominant in cooler and more hydrated magmas, where SO_2 will be converted to H_2S (fig. 19).

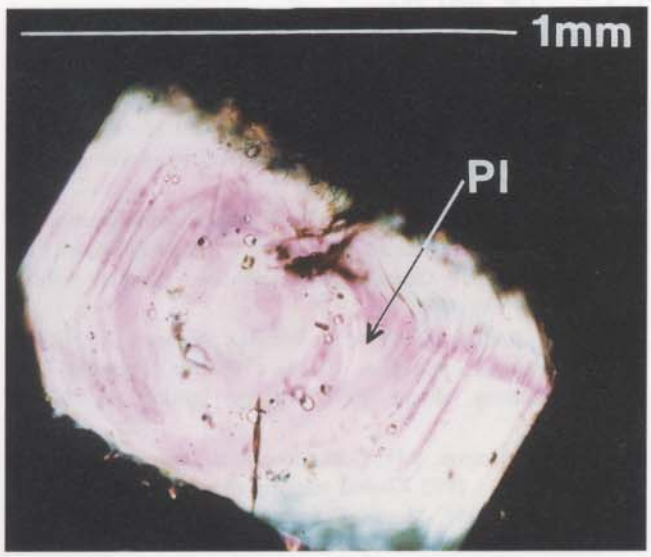

Figure 20. Transmitted light photomicrograph of fluid inclusions in plagioclases (Pl) in dacitic pumice. The inclusions usually occur near the rims of phenocrysts, but some occur in the center of phenocrysts, as shown here.

Underlying mafic magmas at Pinatubo likely released SO_2-rich supercritical fluids during their ascent. The fluids were likely absorbed by the overlying semisolidified dacitic magma. As dacitic magma is cooler and more hydrated than mafic magma, SO_2 would be converted to H_2S (fig. 19). The net effect is oxidation of the dacitic magma. The H_2S produced in the dacitic magma would form sulfides in the dacite melt (stage II of fig. 18) together with elements transported by the fluids, such as Zn, Cd, Cu, and Se. Continual addition of SO_2 would cause further oxidation of the dacitic magma, desulfidation of sulfides, and crystallization of anhydrite.

Sulfur isotopic data of the eruption products support both models. A variation in $\delta^{34}S$ values for individual grains of anhydrite (+3 to +16 ‰; McKibben and others, 1992; this volume) appears to support the incorporation of various types of sulfur from host rocks. Most $\delta^{34}S$ values are in a range between +6 and +8 (Knittel and others, 1992; McKibben and others, 1992; this volume; Bernard and others, this volume). Sulfates formed by hydrolysis of SO_2 have similar $\delta^{34}S$ values (Hattori and Cameron, 1986). The isotopic compositions outside this range could be attributed to a fluctuation in $\delta^{34}S$ of gases discharged from mafic magma, because $\delta^{34}S$ values of sulfur gases released from melt vary, depending upon temperature, f_{O_2}, and f_{H_2O} of the melts (Ueda and Sakai, 1984). Apparent isotopic equilibrium between sulfide and anhydrite in the dacitic magma (McKibben and others, this volume) may be attributed to the isotopic equilibration of sulfur between H_2S and SO_2 in the gas.

At present, there is no evidence to reject the former model, but the latter model is favored because of abundant occurrences of fluid inclusions in the phenocryst rims of hornblende, plagioclase, and quartz in the dacitic pumice (fig. 20), and because of $^{87}Sr/^{86}Sr$ ratios of anhydrite. Phenocrysts contain numerous fluid inclusions, some of which are high in CO_2. They most commonly align with growth bands of phenocrysts near rims. The occurrence supports that fluid percolation from mafic melt into dacitic melt started while phenocrysts were still being formed in the dacitic magma chamber.

As mentioned, $^{87}Sr/^{86}Sr$ ratios of anhydrite are identical to the bulk rocks (this study), whereas alteration products (epidote and anhydrite) have various $^{87}Sr/^{86}Sr$ ratios, up to 0.708 (Hattori and others, 1992).

The percolation of supercritical fluid is also in accord with the occurrence of copper-rich sulfides and their trace elements in the glass. When fluid separation takes place in silicate melts, volatiles such as Se and Cl are enriched in the fluid phase (Greenland and Aruscavage, 1986; Candela and Holland, 1984). Metals that have affinity with these volatiles are also enriched in the fluid. Experimental studies document preferential incorporation of copper into a fluid (Candela and Holland, 1984; Urabe, 1985). Significant copper and zinc are also recorded in volcanic gases emanating from silicate magma (Mizutani, 1970). The enrichment of copper in the upper part of a magma chamber is attributed to vapor transport (Lowenstern and others, 1991). Other elements that have affinity with Cl, such as Cd, Zn, and Ag, are known to be incorporated into a fluid phase (Symonds and others, 1990).

ORIGIN OF SULFUR DISCHARGED TO THE STRATOSPHERE

Various models have been proposed for the origin of sulfur discharged to the stratosphere: (1) breakdown of anhydrite in the magma (Rutherford and Devine, 1991; Baker and Rutherford, 1992), (2) breakdown/absorption of sulfides in melts (Whitney, 1992), and (3) release of gas present in a separate vapor phase (Westrich and Gerlach, 1992). The lack of reaction rims around anhydrite in dacitic pumices argues against the first model. It is also difficult to envisage a conversion of sulfur from a solid phase to SO_2 even at magmatic temperatures in the short period during the height of eruption. In addition, thin reaction rims of sulfides and preservation of most sulfides in the glass phase are not in accord with the second hypothesis. The occurrence of sulfur-bearing phases documented in this paper support the proposal by Westrich and Gerlach (1992) that the SO_2 was most likely derived by release of sulfur present in a vapor phase in the melt.

SUMMARY

The presence of globular and irregularly shaped sulfides in all types of eruption products indicates that an immiscible sulfide liquid formed in the silicate melts during phenocryst crystallization, that sulfur in the melt at that time was predominantly S^{2-}, and that f_{O_2} was below the sulfide/sulfate redox boundary. Later formation of anhydrite in the dacitic melt required oxidation of the melt, as well as addition of sulfur from an external source. High concentrations of Cu, Zn, and Se in late-formed sulfides suggest addition of these elements together with sulfur. It is proposed that the dacitic melt incorporated a supercritical fluid from the underlying mafic magma. The fluid had high SO_2/H_2S and was enriched in volatile and chalcophile metals. Conversion of SO_2 to H_2S in cool, hydrated dacitic magma caused oxidation of the dacitic magma chamber. While f_{O_2} was still below the redox boundary, Cu-rich sulfides formed in the melt. Once f_{O_2} became higher than the redox boundary, incorporation of sulfur into the dacitic magma caused crystallization of anhydrite.

ACKNOWLEDGMENTS

The author thanks R.S. Punongbayan for providing the lodging and transportation for the author's field work, C.G. Newhall and his family for their hospitality at Clark Air Base and their assistance for sampling in the summer of 1992, Ulrich Knittel (Institut für Mineralogie und Lagerstättenlehre, Technische Hochschule Aachen) for providing samples, H.P. Ferrer (Philippine National Oil Company) for permission to examine thin sections and for provision of drill chips in the area, H.G. Aniceto-Villarosa for assisting the examination of drill chip samples, Peter Jones (Ottawa-Carleton Geoscience Centre) for his superb operation of the SEM laboratory, and J.L. Campbell and W.J. Teesdale (Guelph University) for assisting in PIXE analysis. Comments by E.M. Cameron (Geological Survey of Canada), J.A. Donaldson (Ottawa-Carleton Geoscience Centre), J.H. Fournelle (Johns Hopkins University/University of Wisconsin, Madison), Ulrich Knittel, J.F. Luhr (Smithsonian Institution), M.A. McKibben (University of California, Riverside), N. Metrich (Centre National de la Recherche Scientifique, Saclay, France), and C.G. Newhall (USGS) are greatly appreciated. The project was supported by a grant from Natural Science and Engineering Research Council of Canada.

REFERENCES CITED

Andersen, D.J., Lindsley, D.H., and Davidson, P.M., 1993, QUILF: A PASCAL program to assess equilibria among Fe-Mg-Ti oxides, pyroxenes, olivine and quartz: Computers in Geosciences, v. 19, p. 1333–1350.

Anderson, A.T., 1974, Chlorine, sulfur and water in magmas and oceans: Geological Society of America Bulletin, v. 85, p. 1485–1492.

Baker L., and Rutherford, M.J., 1992, Anhydrite breakdown as a possible source of excess Sulfur in the 1991 Mount Pinatubo eruption [abs.]: Eos, Transactions, American Geophysical Union, v. 73, no. 43, p. 625.

Bernard, A., DeMaiffe, D., Mattielli, N., and Punongbayan, R.S., 1991, Anhydrite-bearing pumice from Mount Pinatubo: Further evidence for the existence of sulfur-rich magmas: Nature, v. 354, p. 139–140.

Bernard, A., Knittel, U., Weber, B., Weis, D., Albrecht, A., Hattori, K., Klein, J., and Oles, D., this volume, Petrology and geochemistry of the 1991 eruption products of Mount Pinatubo.

Bluth, G.J.S., Doiron, S.D., Schnetzler, C.C., Krueger, A.J., and Walter, L.S., 1992, Global tracking of the SO_2 clouds from the June 1991 Mount Pinatubo eruptions: Geophysical Research Letters, v. 19, p. 151–154.

Buchanan, D.L., and Nolan, J., 1979, Solubility of sulfur and sulfide immiscibility in synthetic tholeiitic melts and their relevance to Bushveld Complex rocks: Canadian Mineralogist, v. 17, p. 483–494.

Burnham, C.W., and Ohmoto, H., 1980, Late-state processes of felsic magmatism: Society of Mining Geologists of Japan Special Issue, v. 8, p. 1–11.

Cabri, L.J., Blanck, H., El Goresy, A., LaFlamme, J.H.G., Nobiling, R., Sizgoric, M.B., and Traxel, K., 1984, Quantitative trace-element analyses of sulfides from Sudbury and Stillwater by proton microprobe: Canadian Mineralogist, v. 22, p.521–542.

Campbell, J.L., Maxwell, J.A., Teesdale, W.J., Wang, J.X., and Cabri, L.J., 1989, Micro-PIXE as a complement to electron probe microanalysis in mineralogy: Nuclear Instruments and Methods in Physics Research, section B, v. 44, p. 347–356.

Candela, P.A., and Holland, H.D, 1984, The partitioning of copper and molybdenum between melts and aqueous fluids: Geochimica et Cosmochimica Acta, v. 48, p. 373–380.

Carroll, M.R., and Rutherford, M.J., 1988, Sulfur speciation in hydrous experimental glasses of varying oxidation state: Results from measured wavelength shifts of sulfur X-rays: American Mineralogist, v. 73, p. 845–849.

Czamanske, G.K., Kunilov, V.E., Zientek, M.L., Cabri, L.J., Likhachev, A.P., Calk, L.C., and Oscarson, R.L., 1992, A proton-microprobe study of magmatic sulfide ores from the Noril'sk-Talnakh district, Siberia: Canadian Mineralogist, v. 30, p. 249–287.

Delfin, F.G., Jr., 1984, Geology and geothermal potential of Mt. Pinatubo: Philippine National Oil Company, unpublished report, 36 p.

Delfin, F.G., Jr., Villarosa, H.G., Layugan, D.B., Clemente, V.C., Candelaria, M.R., Ruaya, J.R., this volume, Geothermal exploration of the pre-1991 Mount Pinatubo hydrothermal system.

Desborough, G.A., Anderson, A.T., and Wright, T.L., 1968, Mineralogy of sulfides from certain Hawaiian basalts: Economic Geology, v. 63, p. 636–644.

Fournelle, J.H., 1991, Anhydrite and sulfide in pumices from the 15 June 1991 eruption of Mount Pinatubo: Initial examination

[abs.]: Eos, Transactions, American Geophysical Union, v. 72, p. 68.

Francis, R.D., 1990, Sulfide globules in mid-ocean ridge basalts (MORB) and the effect of oxygen abundance in Fe-S-O liquids on the ability of those liquids to partition metals from MORB and komatiite magmas: Chemical Geology, v. 85, p. 199–213.

Frost, B.R., and Lindsley, D.H., 1991, Occurrence of iron-titanium oxides in igneous rocks, *in* Lindsley, D.H., ed., Oxide minerals: Petrologic and magnetic significance: Mineralogical Society of America, Reviews in Mineralogy, v. 25, p. 433–468.

——1992, Equilibria among Fe-Ti oxides, pyroxenes olivine, and quartz, pt. II. Application: American Mineralogist, v. 77, p. 1004–1020.

Gerlach, T.M., 1986, Exsolution of H_2O, CO_2, and S during eruptive episodes at Kilauea volcano, Hawaii: Journal of Geophysical Research, v. 91, p. 12177–12185.

Gleason, J.F., Bhartia, P.K., Herman, J.R., McPeters, R., Newman, P., Stolarski, R.S., Flynn, L., Labow, G., Larko, D., Seftor, C., Wellemeyer, C., Komhyr, W.D., Miller, A.J., and Planet, W., 1993, Record low global ozone in 1992: Science, v. 260, p. 523–526.

Grant, W.B., Browell, E.V., Fishman, J., Brackett, V.G., Fenn, M.A., Butler, C.F., Myor, S.D., Nowicki, G.D., Veiga, R.E., Nganga, D., Minga, A., and Cros, B., 1992, Perturbation of tropical stratospheric ozone by Mt. Pinatubo aerosols-Experimental data [abs.]: Eos, Transactions, American Geophysical Union, v. 73, no. 14, p. 632.

Greenland, L.P., and Aruscavage, P., 1986, Volcanic emission of Se, Te and As from Kilauea volcano, Hawaii: Journal of Volcanology and Geothermal Research, v.27, p. 195–201.

Hamlyn, P.R., and Keays, R.R., 1986, Sulfur saturation and second-stage melts: application to the Bushveld platinum metal deposits: Economic Geology, v. 81, p. 1431–1445.

Hammond, P.A., and Taylor, L.A., 1982, The ilmenite/titanomagnetite assemblage: Kinetics of reequilibration: Earth and Planetary Sciences Letters, v. 61, p. 143–150.

Hattori, K., 1993, High-sulfur magma, a product of fluid discharge from underlying mafic magma: Evidence from Mount Pinatubo, Philippines: Geology, v. 21, p. 1083–1086.

Hattori, K., Arai, S., Francis, D.M., and Clarke, D.B., 1992, Variations of siderophile and chalcophile trace elements among mantle-derived sulfides detected by in-situ micro-PIXE analysis [abs.]: Eos, Transactions, American Geophysical Union, v. 73, no. 14, p. 344.

Hattori, K., and Cameron, E.M., 1986, Archaean magmatic sulphate: Nature, v. 319, p. 45–47.

Heming, R.F., and Carmichael, I.S.E., 1973, High-temperature pumice flows from the Rabaul caldera, Papua New Guinea: Contributions to Mineralogy and Petrology, v. 38, p. 1–20.

Holloway, J.R., 1976, Fluids in the evolution of granitic magmas: Consequences of finite CO_2 solubility: Geological Society of America Bulletin, v. 87, p. 1513–1518.

Imai, A., Listanco, E.L., and Fujii, T., 1992, Petrographic and sulfur isotopic significance of highly oxidized and sulfur-rich magma of Mt. Pinatubo, Philippines [abs.]: Abstracts, International Scientific Conference on Mt. Pinatubo, Manila, 27–30 May 1992, p. 6–7.

———this volume, Highly oxidized and sulfur-rich dacitic magma of Mount Pinatubo: Implication for metallogenesis of porphyry copper mineralization in the Western Luzon arc.

Johnston, A.D., and Stout, J.H., 1984, Development of orthopyroxene-Fe/Mg ferrite symplectites by continuous olivine oxidation: Contributions to Mineralogy and Petrology, v. 88, p. 196–202.

Katsura, T., and Nagashima, S., 1974, Solubility of sulfur in some magmas at 1 atm: Geochimica et Cosmochimica Acta, v. 38, p. 517–531.

Knittel, U., Hattori, K., Hoefs, J., and Oles, D., 1992, Isotopic compositions of anhydrite phenocryst-bearing pumices from the 1991 eruption of Mount Pinatubo, Philippines [abs.]: Eos, Transactions, American Geophysical Union, v. 73, no. 14, p. 342.

Knittel, U., Oles, D., Forster, H., and Punongbayan, R.S., 1991, Pinatubo pumice contains anhydrite [abs.]: Eos, Transactions, American Geophysical Union, v. 72, p. 522.

Lowenstern, J.B., Mahood, G.A., Rivers, M.L., and Sutton, S.R., 1991, Evidence for extreme partitioning of copper into a magmatic vapor phase: Science, v. 252, p. 1405–1409.

Luhr, J.F., Carmichael, I.S.E., and Varekamp, J.C., 1984, The 1982 eruptions of El Chichón volcano, Chiapas, Mexico: Mineralogy and petrology of the anhydrite-bearing pumices: Journal of Volcanology and Geothermal Research, v. 23, p. 69–108.

Mathez, E.A., 1976, Sulfur solubility and magmatic sulfides in submarine basalt glass: Journal of Geophysical Research, v. 81, p. 4269–4276.

Matthews, S.J., Jones, A.P., and Bristow, C.S., 1992, A simple magma-mixing model for sulphur behavior in calc-alkaline volcanic rocks: Mineralogical evidence from Mount Pinatubo 1991 eruption: Journal of the Geological Society of London, v. 149, p. 863–866.

Maxwell, J.A., Campbell, J.L., and Teesdale, W.J., 1989, The Guelph PIXE software package: Nuclear Instruments and Methods in Physics Research, section B, v. 43, p. 218–230.

McKibben, M.A., Eldridge, C.S., and Reyes, A.G., 1992, Multiple origins of anhydrite in Mt. Pinatubo pumice [abs.]: Eos, Transactions, American Geophysical Union, v. 73, p. 633–634.

———this volume, Sulfur isotopic systematics of the June 1991 Mount Pinatubo eruptions: A SHRIMP ion microprobe study.

Measures, C.I., McDuff, R.E., and Edmond, J.M., 1980, Selenium redox chemistry at GEOSECS 1 re-occupation: Earth and Planetary Science Letters, v. 49, p. 102–108.

Mizutani, Y., 1970, Copper and zinc in fumarolic gases of Showashinzan volcano, Hokkaido: Geochemical Journal (Japan), v. 4, p. 87–91.

Morse, S.A., 1980, Kiplapait mineralogy, II: Fe-Ti oxide minerals and the activities of oxygen and silica: Journal of Petrology, v. 21, p. 685–719.

Nagashima, S., and Katsura, T., 1973, The solubility of sulfur in Na_2O-SiO_2 melts under various oxygen partial pressures at 1100°C, 1250°C and 1300°C: Bulletin of Chemical Society of Japan, v. 46, p. 3099–3103.

Pallister, J.S., Hoblitt, R.P., and Reyes, A.G., 1992, A basalt trigger for the 1991 eruptions of Pinatubo volcano?: Nature, v. 356, p. 426–428.

Rajamani, V., and Naldrett, A.J., 1978, Partitioning of Fe, Co, Ni and Cu between sulfide liquid and basaltic melts and the

composition of Ni-Cu sulfide deposits: Economic Geology, v. 73, p. 82–93.

Ruaya, J.R., Ramos, M.N., and Gonfiantini, R., 1992, Assessment of magmatic components of the fluids at Mt. Pinatubo volcanic-geothermal system, Philippines from chemical and isotopic data: Report of the Geological Survey of Japan, v. 279, p. 141–151.

Rutherford, M.J., and Devine, J.D., 1991, Pre-eruption conditions and volatiles in the 1991 Pinatubo magma [abs.]: Eos, Transactions, American Geophysical Union, v. 72, p. 62.

Rye, R.O., Luhr, J.F., and Wasserman, M.D., 1984, Sulfur and oxygen isotopic systematics of the 1982 eruptions of El Chichón volcano, Chiapas, Mexico: Journal of Volcanology and Geothermal Research, v. 23, p. 109–123.

Sillitoe, R.H., and Gappe, I.M., Jr., 1984, Philippine porphyry copper deposits: Geologic setting and characteristics: Committee for Coordination of Joint Prospecting for Mineral Resources in Asian Offshore Areas (CCOP) Project Office Technical Paper 14, 89 p.

Symonds, R.B., Rose, W.I., Gerlach, T.M., Briggs, P.H., and Harmon, R.S., 1990, Evaluation of gases, condensates, and SO_2 emissions from Augustine volcano, Alaska: The degassing of a Cl-rich volcanic system: Bulletin of Volcanology, v. 52, p. 355–374.

Ueda, A., and Itaya, T., 1981, Microphenocrystic pyrrhotite from dacite rocks of Satsuma-Iwojima, Southwest Kyushu, Japan and the solubility of sulfur in dacite magma: Contributions Mineralogy and Petrology, v. 78, p. 21–26.

Ueda, A., and Sakai, H., 1984, Sulfur isotope study of Quaterna volcanic rocks from the Japanese Islands Arc: Geochimica Cosmochimica Acta, v. 48, p. 1837–1848.

Urabe, T., 1985, Aluminous granite as a source magma of hydr thermal ore deposits: An experimental study: Econom Geology, v. 80, p. 148–157.

Wallace, P., and Carmichael, I.S.E., 1992, Sulfur in basaltic ma mas: Geochimica et Cosmochimica Acta, v. 56, p. 1863–1874.

Wedepohl, K.L., ed., Handbook of geochemistry, 1972, ch. 3 Selenium: New York, Springer-Verlag, v. II–3, 34 B–O.

Westrich, H.R., and Gerlach, T.M., 1992, Magmatic gas source f the stratospheric SO_2 cloud from the June 15, 1991, eruptic of Mount Pinatubo: Geology, v. 20, p. 867–870.

Whitney, J.A., 1984, Fugacities of sulfurous gases in pyrrhotit bearing silicic magmas: American Mineralogist, v. 69, p. 69–78.

———1992, Origin and evolution of sulfur in silicic magm [abs.]: Eos, Transactions, American Geophysical Unio v. 73, no. 14, p. 366–367.

Whitney, J.A., and Stormer, J.C., Jr., 1983, Igneous sulfides in th Fish Canyon Tuff and the role of sulfur in calc-alkaline ma mas: Geology, v. 11, p. 99–102.